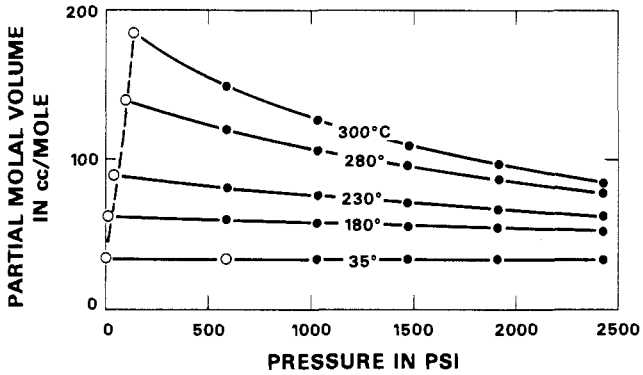

Figure 14. Partial molal volumes of hydrogen, at infinite dilution, in liquid 1,4-diethylbenzene.

those covered by experimental data. The filled-in circles involve only linear extrapolations to $x_2 = 0$, at a constant pressure, within the pressure range of the measurements. Surprisingly, at the lower pressures and higher temperatures, the partial molal volumes of hydrogen are often larger than those of hydrocarbons.

Registry No. Hydrogen, 1333-74-0; *n*-pentane, 109-66-0; 2,3-dimethylbutane, 79-29-8; cyclohexane, 110-82-7; *n*-decane, 124-18-5; *m*-xylene, 108-38-3; 1,4-diethylbenzene, 105-05-5; 1-methylnaphthylene, 90-12-0.

Literature Cited

(1) Connolly, J. F. *J. Chem. Phys.* **1962**, *36*, 2897.
(2) Connolly, J. F. *Proc. Am. Pet. Inst.* **1965**, *45*, III, 62.
(3) Connolly, J. F.; Kandalic, G. A. *Chem. Eng. Prog. Symp. Ser.* **1963**, *59*, 8.
(4) Rossini, F. D.; Pitzer, K. S.; Arnett, R. L.; Braum, R. M.; Pimentel, G. C. *Selected Values of Physical and Thermodynamic Properties of Hydrocarbons and Related Compounds*; Carnegie: Pittsburgh, 1953.

Received for review May 8, 1985. Accepted April 28, 1986.

Supplementary Material Available: Experimental values for solution dilation (13 pages). Ordering information is given on any current masthead page.

Solidification Behavior of the Cinnamic Acid–*p*-Nitrophenol Eutectic System

N. Bahadur Singh* and P. Kumar

Chemistry Department, Gorakhpur University, Gorakhpur 273 009, India

The solid–liquid equilibrium of the cinnamic acid–*p*-nitrophenol (CA–pNP) eutectic system has been investigated. Heat of fusion, microstructure, and strength measurements have been made. Infrared spectral studies indicate molecular association in the formation of the eutectic. Thermodynamic functions such as h^E, g^E, and S^E have been calculated and were found to be negative except g^E. Statistical mechanical treatment shows that the surface nucleation theory holds good in the solidification of the present eutectic.

Introduction

Solid materials are of considerable interest both from the fundamental and from the technological point of view. Eutectic materials also come in this category. In order to control the properties of such materials, studies of phase diagram, linear velocity of crystallization, microstructure, compressive strength, and thermodynamic properties are essential (*1*). The present paper describes the chemistry of the cinnamic acid–*p*-nitrophenol (CA–pNP) eutectic system with reference to the above properties.

Experimental Section

Materials and Purification. *p*-Nitrophenol (BDH) and cinnamic acid (BDH) were purified by repeated distillation under reduced pressure. The purity was checked by determining the melting points with the help of a mercury thermometer correct to ±0.1 °C. The melting points are 112.0 and 133.0 °C, respectively. Cinnamic acid is represented as CA and *p*-nitrophenol is represented as pNP.

Phase Diagram and Undercooling Study. The phase diagram of the CA–pNP system has been studied by the thaw melt method (*2*). Mixtures of various compositions were prepared in glass test tubes by repeated heating, chilling, and grinding in a glass mortar. The melting points and thaw points were determined with a mercury thermometer correct to ±0.1 °C. The undercooling study was made in a manner described by Rastogi and Bassi (*3*).

Study of Microstructures. A microscopic method was used for the study of microstructures of components and eutectic. A glass slide was kept in an oven at a temperature higher than the melting points of the eutectic, and a very small amount of the sample was placed on it. As the sample melted completely, the coverslip was glided on it. The slide was allowed to cool and nucleations were started from one side and this was then photographed with a camera under a microscope of desired magnification. The effect of 0.1% 8-hydroxyquinoline and 4-chloroaniline on the microstructure of the eutectic has also been investigated.

Heat of Fusion Measurements. The heats of fusion of the pure components and the eutectic were determined by differential thermal analyzer (Paulik-Paulik-Erdey MOM derivatograph, Hungary) using the method of Vold (*4*). The heating rate was maintained at 2 °C/min, and the temperature was measured by a Pt–Rh thermocouple. From this method only the relative value of the heat of fusion could be determined.

Compressive Strength Measurements. Compressive strengths of components and eutectic in the form of pellets were determined by an universal testing machine. The pellets were prepared by solidifying the molten materials in glass test tubes of uniform diameter and the surfaces were smoothened by rubbing on emery paper. True stress was obtained by dividing the maximum load applied on the pellet (which was capable of breaking the pellet) by the area of the pellet. For calculating true strain, the total number of divisions on the graph (which indicates the maximum compression) was divided by the magnification (magnification was obtained by dividing chart speed by cross head speed) and the value thus obtained was finally divided by the original length of the pellet.

0021-9568/86/1731-0406$01.50/0

Table I. Melting Temperature, Freezing Temperature, and Undercooling Temperature

mole fraction *p*-nitrophenol	temp, °C		
	melting	freezing	supercooling
1.000	112.0	104.5	7.5
0.9000	108.0	102.0	6.0
0.8074	105.5	97.0	8.5
0.7561	103.0	95.5	7.5
0.5900	96.5	89.5	7.0
0.5880	93.0	87.5	5.5
0.5197	102.0	94.5	7.5
0.3659	115.0	107.5	7.5
0.2049	124.5	116.0	8.5
0.1011	129.0	123.5	5.5
1.0000	133.0	128.0	5.0

Table II. Heat of Fusion of Eutectic and Components

system	$(\Delta_f H)_{expt}$, J/mol	$(\Delta_f H)_{mix.law}$, J/mol
p-nitrophenol	30118	
cinnamic acid	22626	
pNP–CA eutectic	71200	27032

Table III. Excess Thermodynamic Functions

system	h^E, J/mol	g^E, J/mol	S^E, J/mol
pNP–CA eutectic	−14069.6	438.3	−39.8

IR Spectral Studies. The IR spectra of the components and the eutectic were recorded in KBr phase with a Perkin Elmer, Accu Lab 9, spectrophotometer.

Results and Discussion

The phase diagram of the CA–pNP system is shown in Figure 1. The undercooling data are also given in the same figure. The melting points and undercooling data for the mixtures are given in Table I. The thermodynamic analysis shows that the system is nonideal.

The heats of fusion of CA–pNP eutectic system is given in Table II. In the same table the heat of fusion values as calculated from mixture law are also given. As soon as the eutectic melts, there is a considerable possibility of heat of mixing and association, which may result in violation of the mixture law. For this reason excess thermodynamic functions such as excess heat of mixing h^E, entropy of mixing S^E, and free energy of mixing g^E have been calculated (*5*) and are given in Table III.

The eutectic temperature and composition were determined from the phase diagram, and the activity coefficients for components 1 and 2 are calculated from eq 1 where x_i^1 is the mole

$$-\ln x_i^1\gamma_i^1 = \frac{\Delta_f H_i^\circ}{R}\left(\frac{1}{T}-\frac{1}{T_i^0}\right) \tag{1}$$

fraction of component i in the liquid phase, γ_i^1 is the activity coefficient of component i, T is the eutectic temperature, T_i^0 is the melting temperature of component i, $\Delta_f H_i^\circ$ is the heat of fusion, and R is the gas constant. After the eutectic composition, temperature, and activity coefficient were known, the excess thermodynamic functions were calculated by using eq 2–4 where R is a gas constant, T is the freezing temperature.

$$g^E = RT(x_1 \ln \gamma_1 + x_2 \ln \gamma_2) \tag{2}$$

$$S^E = -R\left(x_1 \ln \gamma_1 + x_2 \ln \gamma_2 + x_1 T\frac{\partial \ln \gamma_1}{\partial T} + x_2 T\frac{\partial \ln \gamma_2}{\partial T}\right) \tag{3}$$

$$h^E = -RT^2\left(x_1\frac{\partial \ln \gamma_1}{\partial T} + x_2\frac{\partial \ln \gamma_2}{\partial T}\right) \tag{4}$$

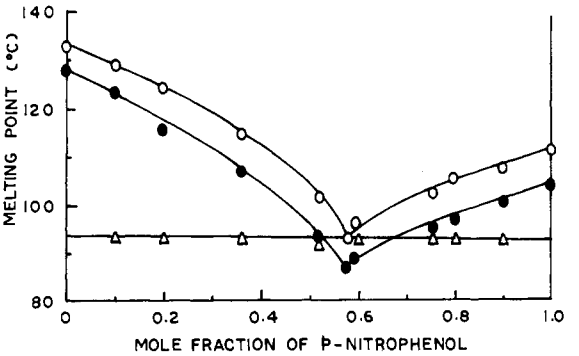

Figure 1. Phase diagram for the *p*-nitrophenol–cinnamic acid eutectic system: O, melting temperature; Δ, thaw temperature; ●, freezing temperature.

The values of $\partial \ln \gamma_i/\partial T$ were determined from the slopes of the liquidus curves in the phase diagrams in the following manner.

On differentiating eq 1, one would get

$$-\frac{1}{x_i}\frac{\partial x_i}{\partial T} - \frac{\partial \ln \gamma_i}{\partial T} = \frac{-\Delta_f H_i^\circ}{RT^2} \tag{5}$$

or

$$x_i\frac{\partial \ln \gamma_i}{\partial T} = x_i\frac{\Delta_f H_i^\circ}{RT^2} - \frac{\partial x_i}{\partial T} \tag{6}$$

Since the liquidus curves in the phase diagrams are straight in the region of eutectic composition, the value of $\partial x_i/\partial T$ can be calculated with accuracy, using eq 6.

The values of excess thermodynamic functions are given in Table III. The values of the excess functions except g^E are negative. This indicates that the interaction between unlike molecules is stronger than between the like molecules.

The heats of fusion of components and eutectics determined experimentally are given in Table II. If the eutectics were a simple mixture of the two components involving no heat of mixing or any type of association in the melt, the heat of fusion would simply be given by

$$(\Delta_f H)_e = x_1\Delta_f H_1 + x_2\Delta_f H_2 \tag{7}$$

where x_1 and x_2 are the mole fractions of components 1 and 2, respectively. $\Delta_f H_1$ and $\Delta_f H_2$ are the heats of fusion of components 1 and 2, respectively. The heat of fusion value calculated from eq 7 for the eutectic is also given in Table II and is much lower than the experimental value. This indicates that eutectic is not simply a mechanical mixture of the two components but there is some type of interaction and for this reason, the heat of fusion of the eutectic is considerably higher than the sum of the components.

The infrared spectra of components and eutectic are given in Figure 2. The OH stretching frequency in the components come at around 3500 cm^{-1} whereas in the case of eutectic the intensity of this peak is reduced considerably. This shows that in the eutectic the OH group is associated. This confirms that there is some interaction between the components during the formation of eutectic mixture.

The microstructure of CA is completely irregular whereas that of pNP is regular and the crystallization starts from a point and grows in the form of a web. The microstructure of eutectic is very interesting. The two phases are quite distinct. The CA crystallizes in the form of a regular parallelogram and pNP in the form of feathers. It appears that in the eutectic both the components influence the mode of crystallization of each other and the crystallization front is regular with a flat surface. This regularity may give higher compressive strength which we shall discuss later on. In the presence of impurities the micros-

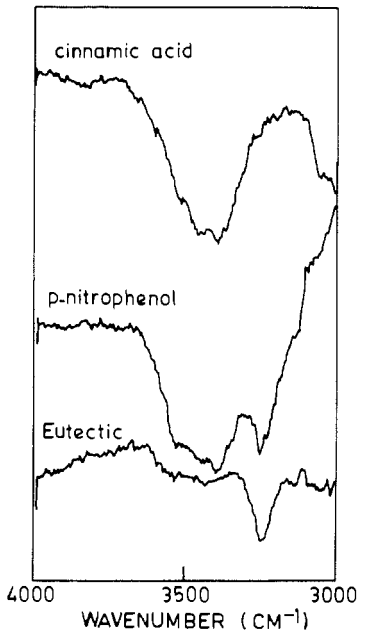

Figure 2. Infrared spectra of *p*-nitrophenol–cinnamic acid eutectic, *p*-nitrophenol, and cinnamic acid.

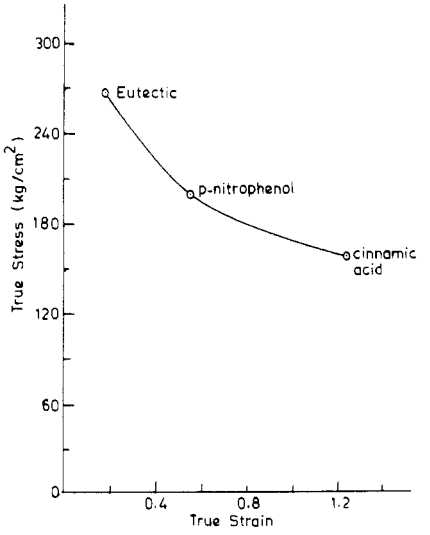

Figure 3. Stress–strain variation.

tructure is changed completely. The flat crystal surfaces of CA disappear and it becomes microcrystalline.

During the solidification process, the molecules lose rotational, positional, and configurational entropy, so that their arrangement at the liquid–solid interface may be just as important as the number of molecules present. This in turn implies that molecular crystals usually have high entropies of melting and according to theories of interface morphology, higher entropies of melting can be associated with an atomically flat crystal face. Jackson (*6*) has presented a statistical model in which the interface roughness is defined in terms of a parameter α, which is given by

$$\alpha = \xi \frac{\Delta_f H}{RT_m} \tag{8}$$

where ξ is a geometrical coefficient which generally lies between $^1/_2$ and 1. When $\xi = 1$, flat crystal surfaces are essential with $\alpha > 2$. In the present case, $\alpha = 23.4$, which shows that surface nucleation theory (*7*) holds good in the present eutectic system.

In order to assess the regularity of structure and its effect on material property, the compressive strengths of the eutectic and the components have been measured. Compressive strength measurements show that the eutectic has the highest strength as compared to the components. This further confirms the regularity of structure and association of molecules in the eutectic. In Figure 3, the stress–strain relationship is given, which shows that the eutectic has the highest stress even at a lower strain.

Acknowledgment

We are thankful to Prof. S. C. Tripathi, Head, Chemistry Department, for providing laboratory facilities.

Registry No. CA, 621-82-9; pNP, 100-02-7.

Literature Cited

(1) Singh, N. B.; Dwivedi, K. D. *J. Sci. Ind. Res.* **1982**, *41*, 98.
(2) Rastogi, R. P.; Varma, K. T. R. *J. Chem. Soc.* **1956**, 2097.
(3) Rastogi, R. P.; Bassi, P. S. *J. Phys. Chem.* **1964**, *68*, 2398.
(4) Vold, M. J., *Anal. Chem.* **1949**, *21*, 683.
(5) Rastogi, R. P.; Singh, N. B.; Rastogi, P.; Singh, N. B. *J. Cryst. Growth* **1977**, *40*, 234.
(6) Jackson, K. A. *Liquid Metals and Solidification*; American Society of Metals: Cleveland, OH, 1958; p 174.
(7) Sears, G. W. *J. Phys. Chem. Solids.* **1959**, *2*, 37.

Received for review October 21, 1985. Revised manuscript received March 11, 1986. Accepted April 9, 1988. P.K. is thankful to U.G.C., New Delhi, for awarding a fellowship.

Liquid–Liquid Phase Equilibria in the Propylene Carbonate + Methyl Isobutyl Ketone + Water System

Nandani Rajapakse, Harmon L. Finston, and Vojtech Fried*

Chemistry Department, The City University of New York, Brooklyn College, Brooklyn, New York 11210

The mutual solubility of propylene carbonate + methyl isobutyl ketone + water was studied at different temperatures. The temperature effect upon solubility is relatively small.

Introduction

Propylene carbonate (4-methyl-1,3-dioxalan-2-one) is a widely used solvent in extraction and in electrochemical studies (*1–7*). The problem of applying propylene carbonate in industrial processes is its large solubility in water. The purpose of this work

0021-9568/86/1731-0408$01.50/0